

## Article

# Effect of Electron Beam Surface Modification on the Plasticity of Inconel Alloy 625

Stefan Valkov <sup>1,2,\*</sup> , Georgi Kotlarski <sup>1</sup> , Stoyan Parshorov <sup>3</sup>, Maria Ormanova <sup>1</sup>, Borislav Stoyanov <sup>4</sup> , Fatme Padikova <sup>1,2</sup> and Ivan Parshorov <sup>3</sup>

<sup>1</sup> Institute of Electronics, Bulgarian Academy of Sciences, 72 Tzarigradsko Chaussee Blvd., 1784 Sofia, Bulgaria; gvkotlarski@gmail.com (G.K.); m.ormanova@ie.bas.bg (M.O.); f.padikova@yahoo.com (F.P.)

<sup>2</sup> Department of Mathematics, Informatics and Natural Sciences, Technical University of Gabrovo, 4 H. Dimitar Str., 5300 Gabrovo, Bulgaria

<sup>3</sup> Institute of Metal Science, Equipment and Technologies with Hydro- and Aerodynamics Centre, Bulgarian Academy of Sciences, 67 Shipchenski Prohod Blvd., 1574 Sofia, Bulgaria; s\_parshorov@ims.bas.bg (S.P.); parsh@ims.bas.bg (I.P.)

<sup>4</sup> Department of Industrial Design and Textile Engineering, Technical University of Gabrovo, 4 H. Dimitar Str., 5300 Gabrovo, Bulgaria; b.stoyanov@tugab.bg

\* Correspondence: stsvalkov@gmail.com

**Abstract:** In the present work, we present results on the influence of electron beam surface modification on the resistance to plastic deformation and plasticity of Inconel alloy 625. During the treatment procedure, the electron beam currents were 10 and 20 mA, corresponding to beam powers of 600 W and 1200 W. The structures of the modified specimens were studied using X-ray diffraction (XRD), scanning electron microscopy (SEM), and energy-dispersive X-ray spectroscopy (EDX). The nanohardness and Young's modulus were studied through nanoindentation experiments. The plasticity of the treated materials as well as of the untreated ones was studied through an evaluation of  $H^3/E^2$ , which points to resistance to plastic deformation. The results obtained show that the electron beam surface modification procedure leads to a reorientation of microvolumes and the formation of a preferred crystallographic orientation. The surface treatment of the samples using an electron beam with a power of 600 W did not lead to major changes in the structures of the samples. However, the use of a beam with a power of 1200 W led to the formation of a clearly separated modified zone with a thickness in the range of 13 to 15  $\mu\text{m}$ . The Young's modulus increased from about 100 to 153 GPa in the case of electron beam surface modification using the lower-power electron beam. The application of the higher-power electron beam did not lead to a significant change in the modulus of elasticity as compared to the untreated specimen. Also, it was found that the treatment procedure pointed to a decrease in nanohardness when the maximum power of the electron beam was applied. The resistance to plastic deformation, i.e., the  $H^3/E^2$  ratio, showed that the ratio decreased significantly in both cases of electron beam surface modification, pointing to an improvement in the plasticity of the surface of the Inconel alloy 625.

**Keywords:** Inconel alloy 625; electron beam surface modification; resistance to plastic deformation; plasticity; hardness; Young's modulus



**Citation:** Valkov, S.; Kotlarski, G.; Parshorov, S.; Ormanova, M.; Stoyanov, B.; Padikova, F.; Parshorov, I. Effect of Electron Beam Surface Modification on the Plasticity of Inconel Alloy 625. *Coatings* **2024**, *14*, 268. <https://doi.org/10.3390/coatings14030268>

Academic Editor: Hideyuki Murakami

Received: 16 January 2024

Revised: 18 February 2024

Accepted: 21 February 2024

Published: 22 February 2024



**Copyright:** © 2024 by the authors. Licensee MDPI, Basel, Switzerland. This article is an open access article distributed under the terms and conditions of the Creative Commons Attribution (CC BY) license (<https://creativecommons.org/licenses/by/4.0/>).

## 1. Introduction

Nowadays, the methods and techniques for the treatment of structures and surface properties by electron beam modification are considered very promising due to their very short processing times in comparison with those of traditional methods, as well as the very high reproducibility of the technological conditions, the uniform distribution of the energy of the beam, etc. [1,2]. All of these features make the electron beam surface modification technology very attractive for a number of industrial fields, such as aircraft building, automotive production, marine manufacturing, and others [3,4]. Electron beam surface

modification is executed by irradiating the surface of the specimens with a concentrated flow of accelerated electrons. The energy of the electrons is transformed into heat when interacting with the modified materials, and as a result, a thermal field from the top of the surface to the bottom of the specimen is formed. Heating/cooling cycles have a rapid nature and can reach values of  $10^4$ – $10^5$  K/s, which can change chemical compositions and lead to phase changes, the formation of crystallographic texture, etc. [5,6].

The authors of [7,8] have studied the possibility of controlling the structure and properties of tool steels with electron beam treatment technology. They concluded that the mechanical characteristics of the samples were greatly improved after applying the treatment technology due to the formation of a finer microstructure. Rakhadilov et al. [9] studied the effect of the electron beam irradiation and modification of R6M5 steel, and the results showed that the volume fractions, as well as the internal stresses of the  $\alpha'$  lamellar martensitic structure, increased. Zhao et al. [10] have studied the modification of austenitic stainless steel material by an electron beam remelting approach. Their results showed that the tribological properties were improved and the surface roughness was reduced. Similarly, Valkov et al. [11] studied the influence of an electron beam treatment procedure on the corrosion properties of Co-Cr-Mo alloys. The results showed that the aforementioned chemical properties of the alloy were significantly improved after the application of the maximal value of the beam power of 750 W, with the sample moving at a speed of 5 mm/s. The researchers mentioned that the main reasons for this enhancement were the formation of the preferred crystallographic orientation and the elimination of pores, cracks, and other structural defects [11].

It is important to note that Ni-based superalloys, such as Inconel alloys, are very important for modern industry due to their attractive functional and high-temperature properties [12–14]. Inconel alloys have already been well introduced in many industrial branches like aerospace, aircraft, marine, and more [15,16]. The authors of [17] demonstrated the fabrication of an Inconel alloy 718 with a laser power deposition technique, where a novel gradient laser power approach was used. They showed that the proposed approach led to a significant improvement in strength and ductility as compared with the constant laser power deposition technique, where the elongation increased by 18%–83%. Another investigation [18] points out the possibility of improving the plasticity of Inconel alloy 718 by a novel heat treatment approach, including higher-temperature homogenization and a lower-temperature aging treatment. Their results showed that the proposed approach leads to an improvement in the plasticity of the alloy of 41%. The authors of [19] investigated the possibilities of improving the mechanical properties of Inconel alloy 625 by cold rolling and annealing. The results demonstrated an enhancement in yield strength and a significant reduction in plasticity.

In summary, electron beam surface treatment technology is highly applicable for the surface treatment of metallic components in order to improve their structural and mechanical properties. Due to the high integration of Inconel alloys into a large quantity of industrial fields, the possibility of their modification and optimization for specific applications needs to be evaluated. The authors of [20] have studied the microstructure and wear properties of an electron-beam-modified Inconel Ni-based alloy 625, and the results showed that the wear properties were improved due to the strengthening effect of the treatment. However, investigations regarding the effect of treating the surface of Inconel alloys using high-energy fluxes are highly limited regarding the effect of the power of the electron beam on the plasticity of the specimens. Plasticity is one of the most important properties of metals and alloys when they are subjected to shaping and forming procedures. The plasticity and plastic deformation of materials are properties of ductility. Thus, brittle materials cannot be plastically deformed and shaped, which significantly limits their range of applications. Moreover, the improved plasticity of metals and alloys corresponds to an enhancement in their damping properties, reduced crack formation, etc., which could open many practical applications in modern industrial branches.

Therefore, in this study, we propose an investigation of the effect of the power of the electron beam on the microstructure, Young's modulus, hardness, and plasticity of electron-beam-processed Inconel alloys 625. In the present study, the plasticity was studied by the evaluation of the  $H^3/E^2$  ratio, pointing to resistance to plastic deformation.

## 2. Materials and Methods

The studied Inconel alloy 625 specimens had dimensions of  $10 \times 10 \times 5$  mm. The chemical composition of the initial samples is presented in Table 1.

**Table 1.** Chemical composition of the investigated Inconel alloys 625 (in wt.%).

Cr	Mn	Fe	Co	Ni	Mo	W	Ti	Cu	Other
29.5	0.5	7.0	0.2	57.0	3.7	0.2	-	0.2	1.7

The electron beam surface modification procedure was realized on the evoBeam Cube 400 electron beam machine. During the experiments, the accelerating voltage was 60 kV, the speed of the movement of the samples was 40 mm/s, and the electron beam current was chosen to be 10 and 20 mA, corresponding to beam powers of 600 and 1200 W, respectively. The application of these values of the beam current and power was chosen in order to realize a surface modification with and without melting the surface. The application of the lower values of the beam current and power led to a modification without melting the surface, while the use of the higher beam current and power, respectively, led to a modification with the melting of the treated surface. The beam deflection geometry used for these experiments was in the form of a line with a length corresponding to the width of the specimens, i.e., 10 mm. A schematic representation of the electron beam surface modification procedure of the Inconel alloys 625 is shown in Figure 1.

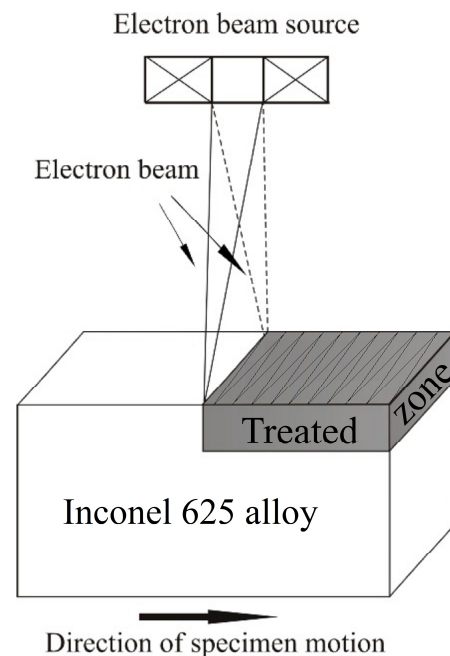


**Figure 1.** A schematic diagram of the electron beam surface modification procedure of Inconel alloys 625.

The phase configuration of the electron-beam-processed specimens, as well as the initial one (untreated), was studied by X-ray diffraction (XRD) experiments. They were realized in the symmetrical Bragg–Brentano mode on a Philips PW1050 (Amsterdam, The Netherlands) X-ray diffractometer with  $\text{CuK}\alpha$ -characteristic radiation ( $1.54 \text{ \AA}$ ). The

measurements were recorded in a range of 35 to 95 degrees, with a step of 0.05° and a counting time of 0.1 s per step.

The structures and contents of chemical elements were studied in detail with a scanning electron microscope (SEM), LYRA I XMU (Tescan), Brno, Czech Republic, equipped with an energy-dispersive X-ray spectroscopy detector used for obtaining information about the chemical composition of the samples.

The surface hardness and Young's modulus were studied by nanoindentation experiments, where a nanomechanical tester (Bruker, Billerica, MA, USA) was employed for the experiments. The measurements consisted of a total of 48 nanoindentations, where the applied load was 50 mN. The resistance to plastic deformation was evaluated via the  $H^3/E^2$  ratio.

### 3. Results

The phase compositions of the untreated Inconel alloys 625 as well as the electron-beam-treated material were studied by X-ray diffraction (XRD) experiments. The experimentally obtained XRD patterns of the initial Inconel alloy 625 as well as the electron-beam-modified alloy with a beam power of 600 and 1200 W are shown in Figure 2. No amorphous-like halos can be observed in any of the considered cases (i.e., in the pattern of the initial alloy or in the diffractograms corresponding to the electron-beam-modified specimens), meaning that the structure of the specimens is fully crystalline, and no amorphous structure can be observed. The experimentally obtained XRD patterns are typical for polycrystalline materials, exhibiting diffraction maxima of the face-centered cubic (FCC) (111), (200), (220), and (311) crystallographic planes of a Ni-Cr solid solution, belonging to the {111}, {100}, {110}, and {311} families of crystallographic planes, respectively. This structure is also known as the  $\gamma$  phase. It was found that the estimated phase composition remains unchanged in all the considered cases, meaning that the electron beam surface treatment procedure using the aforementioned technological conditions and a beam current of 10 and 20 mA, corresponding to a beam power of 600 and 1200 W, does not lead to changes in the above-mentioned structural parameters. It should be noted that the intensities of the observed diffraction maxima significantly differ concerning the initial Inconel alloy 625 as well as the surface-modified material by the scanning electron beam. It is obvious that the intensity of the peak corresponding to the (111) crystallographic plane is the highest in the case of the untreated material. However, the specimen modified by a scanning electron beam using a beam current of 10 mA exhibits a decrease in the intensity of the diffraction peak corresponding to the (111) plane, and the maximum of the (200) plane is characterized by the highest intensity among all the considered peaks. The pattern corresponding to the specimen treated by a scanning electron beam using a beam power of 1200 W exhibits negligible peaks corresponding to the (111) and (200) crystallographic planes, while the maximum of the (220) plane becomes much stronger in comparison with the cases of the initial Inconel alloy 625 as well as of the electron-beam-modified specimen using a beam power of 600 W. All these specific observations point to the formation of a preferred crystallographic orientation and reorientation in the microvolumes within the matrix of the considered Inconel alloy 625. As already mentioned, after the application of these technologies, the heating and cooling rates are quite high (about  $10^4$ – $10^5$  K/s), and these conditions are known as the highly non-equilibrium conditions. The highly non-equilibrium conditions of the used surface modification technique are considered a prerequisite for the formation of a crystallographic texture and preferred crystallographic orientation [11,21]. Moreover, these effects are typical for the electron-beam-modified surfaces of metals and alloys, where similar results are demonstrated in other studies [22].



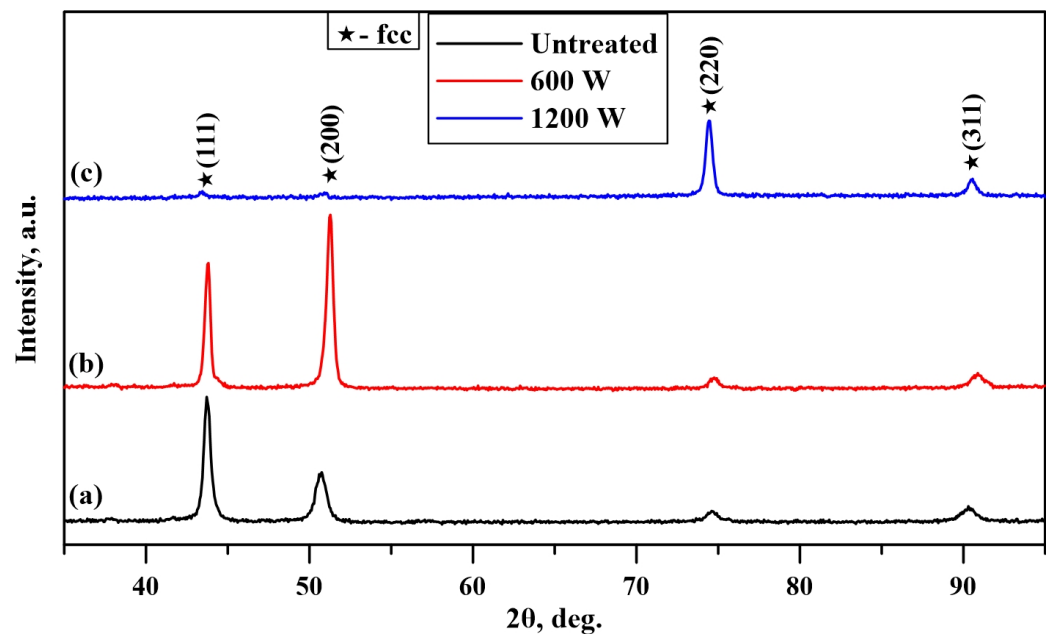


**Figure 2.** X-ray diffraction patterns of (a) Inconel alloy 625; (b) electron-beam-modified specimen with a beam power of 600 W; and (c) electron-beam-modified specimen with a beam power of 1200 W.

Figures 3–5 show cross-sectional SEM images of the considered specimens. Figure 3 exhibits the microstructure of the untreated sample. Figure 4 corresponds to the electron-beam-modified alloy that was modified by a beam current of 10 mA, corresponding to a beam power of 600 W. Figure 5 exhibits cross-sectional images of the sample treated using a 20 mA current electron beam, corresponding to a beam power of 1200 W. Figure 5a presents a low-magnification SEM image, while Figure 5b is a high-magnification micrograph. The chemical compositions of the considered specimens are shown in Table 2. Considering the untreated specimen, it is clear that its microstructure consists of the base Ni-Cr matrix as well as some precipitates that are characterized by an irregular shape. The results indicate that the determined chemical composition of the base matrix matches very well with the data from the manufacturer. However, the elemental compositions of the precipitates exhibit a reduction in the amount of Ni and an increase in iron content. This microstructure is typical for Inconel alloys 625 [23]. The specimen irradiated with a beam current of 10 mA, corresponding to a beam power of 600 W, exhibits a very similar microstructure. No clearly visible modified zone can be distinguished. The precipitates are still characterized by irregular shapes, and no significant refinement can be observed in the microstructure. This means that the value of the beam power of 600 W is insufficient for microstructural modification, and no significant changes in the microstructure can be observed. It is important to note that the chemical composition of the precipitates as well as the base material matrix is very similar to that of the untreated material, meaning that the treatment under the above-mentioned technological conditions does not lead to changes in the elemental composition of the alloy (Table 2).

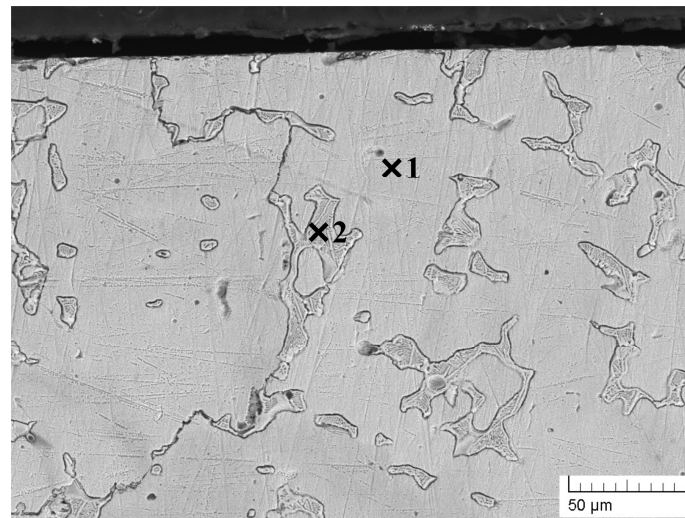


**Figure 3.** Cross section of the untreated Inconel alloy 625.

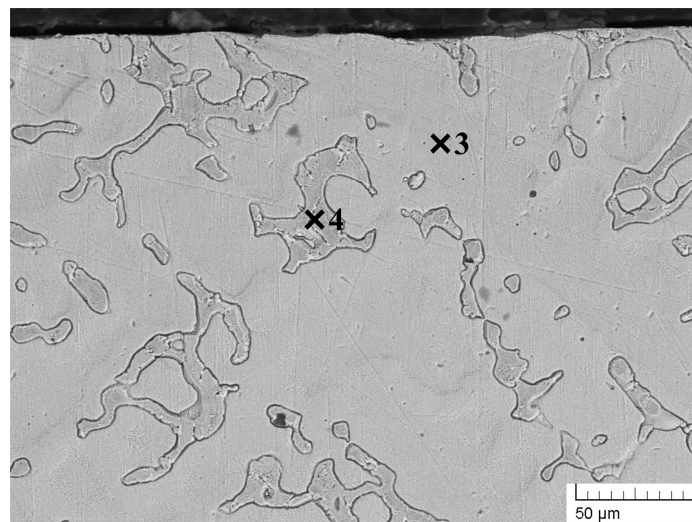


**Figure 4.** Cross section of the Inconel alloy 625 processed using a beam power of 600 W.

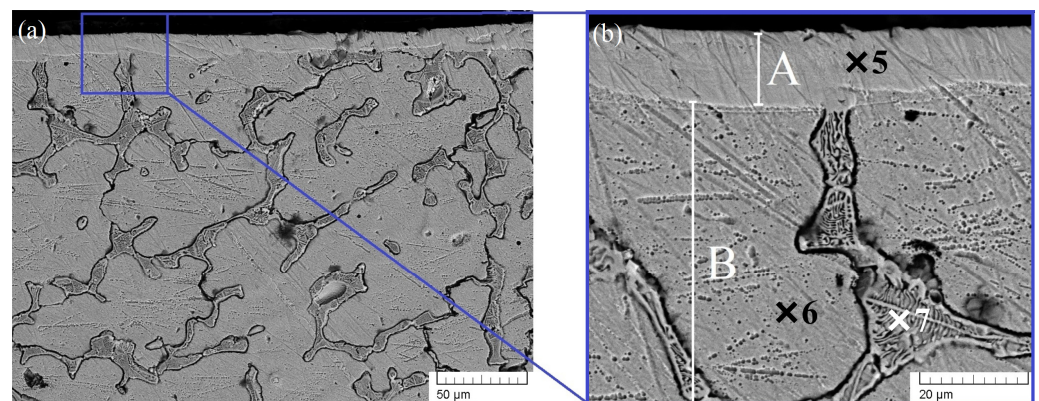


**Figure 5.** Cross section of the Inconel alloy 625 modified by a beam power of 1200 W: (a) low magnification and (b) high magnification.

**Table 2.** Chemical compositions of the untreated and electron-beam-treated Inconel alloys 625 (in wt.%).

Specimen	Point	Cr	Mn	Fe	Ni	Mo
untreated	1	35.3 ± 3.3	4.2 ± 1.1	9.3 ± 1.3	51.3 ± 5.2	0.3 ± 0.1
	2	32.2 ± 2.0	8.3 ± 1.3	23.1 ± 1.6	30.8 ± 2.1	5.6 ± 0.1
600 W	3	34.2 ± 3.0	4.9 ± 1.3	10.1 ± 1.4	50.6 ± 4.5	0.2 ± 0.1
	4	31.2 ± 2.9	7.4 ± 1.4	25.0 ± 1.9	31.9 ± 2.2	4.5 ± 0.1
1200 W	5	34.2 ± 3.6	3.4 ± 1.5	9.0 ± 1.8	52.8 ± 6.1	0.6 ± 0.1
	6	33.8 ± 4.1	4.2 ± 1.3	10.6 ± 1.8	51.1 ± 5.6	0.3 ± 0.1
	7	30.6 ± 3.3	9.1 ± 1.1	24.6 ± 2.0	31.8 ± 3.1	3.9 ± 0.2

Figure 5a presents a low-magnification cross-sectional view of the structure of the sample obtained by surface treatment with an electron beam with a power of 1200 W. The micrograph exhibits a clearly distinguishable modified zone, as well as the untreated material. The higher-magnification image (Figure 5b) shows the modified zone, which is marked as zone A, as well as the base alloy material, indicated as B. The thickness of the modified zone varies from about 13 to 15  $\mu\text{m}$ , where no precipitates can be seen, and a homogeneous structure is obtained on the surface of the Inconel alloy 625. This means that increasing the power of the heat source leads to the dissolution of Mo-rich precipitates. According to the authors of [24], higher currents of the electron beam lead to an increase in the surface temperature of the modified material. Apparently, this increase in the surface temperature was sufficient to cause the dissolution of the precipitates and the formation of a separate molten zone. The EDX results for the chemical composition show that it is very similar to that of the matrix of the alloy and is typical for Ni-based superalloys, where the amount of Ni is predominant. The base alloy material (i.e., under the modified zone) again exhibits a Ni-Cr matrix with randomly distributed Fe-rich precipitates within it. The chemical composition of both—the precipitates and the matrix—is similar to that of the previously investigated specimens, meaning that no significant changes in the microstructure can be observed under the electron-beam-modified zone.

The surface hardness and Young's modulus of the considered specimens were studied by nanoindentation experiments, according to the Oliver Pharr method [25,26]. The load-displacement curves are shown in Figure 6. From the load-displacement curves, it can be seen that the penetration level of the indenter did exceed 1.3  $\mu\text{m}$  in the case of the measurements of the specimen modified by an electron beam with a power of 1200 W. Therefore, the penetration level is within 10% of the melted zone, and the measurements were not influenced by the base matrix of the alloy. The experimentally obtained results are presented in Table 3 and Figure 7. It was found that the hardness of the untreated specimen and that of the specimen treated with a beam current of 10 mA, corresponding to a beam power of 600 W, is the same and is about 3 GPa. However, the application of the modification procedure with a higher beam power led to a decrease in the discussed mechanical characteristic to about 2.5 GPa. As mentioned previously, the application of a higher beam power during the treatment procedure leads to surface melting and the dissolution of precipitates, while the use of a lower one is not enough to melt the surface and dissolve the particulates. This could be considered a reason for the reduction in the hardness of the surface of the specimen treated by a beam power of 1200 W. The Young's modulus of the untreated specimen is about 110 GPa and increases to about 153 GPa after the application of the electron beam modification procedure with the beam power of 600 W. The rise in the modulus of elasticity could be attributed to the formation of a crystallographic texture and the reorientation of microvolumes. It has already been mentioned that the application of this technique for surface modification can form a preferred crystallographic orientation and reorient the microvolumes of the modified material [11,21]. The results of the XRD experiments showed that the intensities of the observed diffraction maxima significantly differ concerning the initial material and electron-beam-surface-modified alloy. Therefore, a

reorientation in the microvolumes occurred after the application of the surface modification procedure with a beam power of 600 W, which could be considered a reason for the rise in the modulus of elasticity. Treating the surface of the samples with a higher-power electron beam led to a decrease in Young’s modulus to 113 GPa, which is closer to the original value of the alloy. The lower modulus of elasticity in the case of electron beam modification using the higher beam power of 1200 W, as compared with the lower beam power of 600 W, could be attributed to the melting of the surface and the formation of the clearly separated melted zone where the precipitates were dissolved. The absence of precipitates in the microstructure of the alloy could be considered a reason for the reduction in the Young’s modulus since there are no obstacles for dislocation movement.

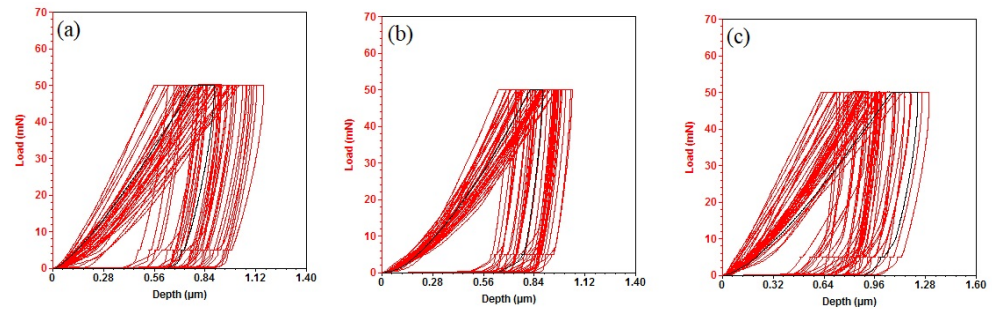


Figure 6. Load–displacement curves of (a) untreated sample; (b) electron-beam-modified sample with a beam power of 600 W; and (c) electron-beam-modified sample with a beam power of 1200 W.

Table 3. Mechanical characteristics of the samples.

Specimen	Hardness (H), GPa	Young’s Modulus (E), GPa	H <sup>3</sup> /E <sup>2</sup> , GPa
Untreated	3.05 ± 1.05	109.95 ± 15.53	0.0023
600 W	3.00 ± 0.70	153.11 ± 14.54	0.0011
1200 W	2.55 ± 0.75	113.53 ± 11.60	0.0013

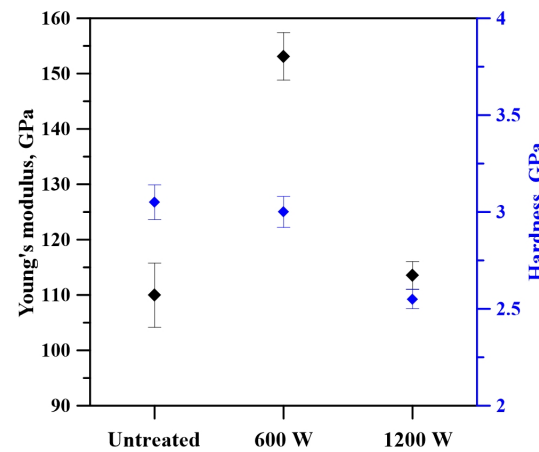
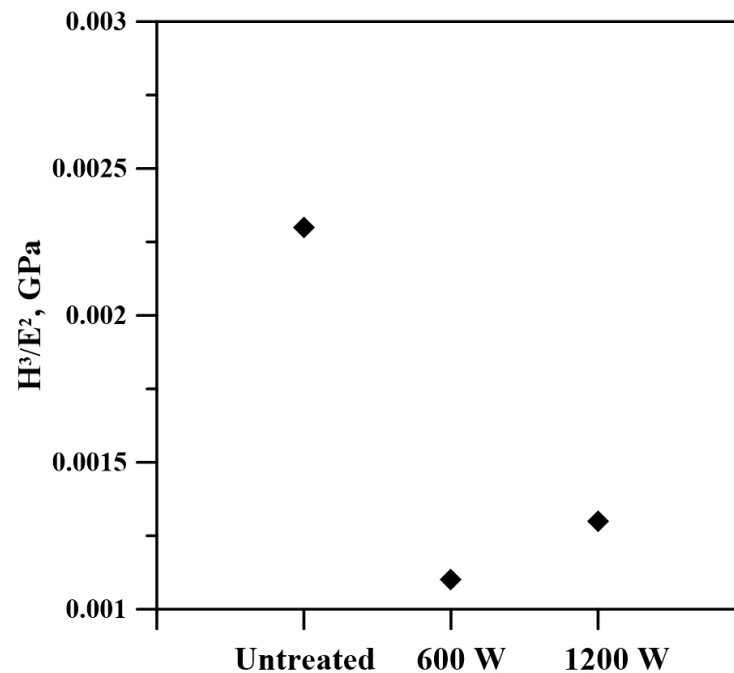


Figure 7. Young’s modulus and hardness of the untreated and treated specimens.

To obtain a better understanding of the plasticity of the Inconel alloy 625 and the influence of the electron beam treatment on plastic deformation, the H<sup>3</sup>/E<sup>2</sup> ratio was evaluated. The ratio H<sup>3</sup>/E<sup>2</sup> signifies the resistance to plastic deformation [27]. The results are presented in Table 2 and Figure 8. Lower values of the H<sup>3</sup>/E<sup>2</sup> ratio point to a lower resistance to plastic deformation, meaning that the modified material can undergo plastic deformation without fracturing [28]. Therefore, a reduction in the H<sup>3</sup>/E<sup>2</sup> ratio and, thus, a reduction in the resistance to plastic deformation lead to an enhancement in the plasticity on the surface of the alloy, which could be considered a significant improvement in its functional properties. The results of this study show that in all the considered cases of



electron beam surface modification of the Inconel alloy 625, the ratio of  $H^3/E^2$  decreases. This means that the plastic deformation resistance decreases, pointing to an enhancement in the plastic properties on the modified surfaces. The measured  $H^3/E^2$  ratio of the untreated alloy is 0.0023 GPa, and it reduces to 0.0011 GPa in the case of electron beam surface modification with a beam power of 600 W (i.e., a decrease of 52%) and to 0.0013 GPa in the case of 1200 W (i.e., a decrease of 43%). Therefore, the plasticity of the alloy improved by more than 50%, which could be useful for a number of potential practical applications in the field of modern industry for the Inconel alloy 625. Plasticity is one of the most important properties of metals and alloys when they are subjected to shaping and forming procedures. The plasticity and plastic deformation of materials are properties of ductility. Thus, brittle materials cannot be plastically deformed and shaped, which significantly limits their range of applications. Moreover, an improved plasticity of metals and alloys corresponds to an enhancement in their damping properties. Also, enhanced plastic properties on surfaces point to a significant reduction in crack formation and initiation, which is also important in a number of practical applications in modern industrial branches. These results could lead to an extension in the range of the current applications of the discussed metallic material as well as open up a number of novel fields of potential practical applications.



**Figure 8.**  $H^3/E^2$  ratios of the untreated Inconel alloy 625 and those surface-treated with beam powers of 600 and 1200 W.

#### 4. Discussion

In this work, the plasticity of Inconel 625 samples was studied as a function of the input power of the electron beam. The plasticity of the material was evaluated through measurements of the hardness and Young's modulus of the modified surfaces and then the ratio  $H^3/E^2$ , which represents the resistance to plastic deformation, i.e., the higher the values of the ratio are, the higher the resistance to plastic deformation is [27]. It was found that after the application of the electron beam surface modification procedure, the  $H^3/E^2$  ratio decreased, pointing to a decrease in the resistance to plastic deformation or an improvement in the plastic properties of the electron-beam-modified surfaces. As already mentioned, the plasticity of the metallic materials can be explained by their ability to be deformed plastically without fracturing, crack formation, etc. In this sense, a crystallographic structure is of major importance for the plasticity and plastic deformation of metallic materials. Plastic deformation is realized by dislocation movement, where slipping



is the main mechanism carried out in a certain slipping system, which is defined by the family of crystallographic planes and the corresponding crystallographic direction [29]. It is known that five independent slip systems are required for deforming metal and alloys plastically without the formation of cracks, fractures, etc. At the same time, a face-centered cubic structure is characterized by 12 independent slip systems, and therefore, these kinds of structures can be characterized by very good plasticity, can be easily shaped and rolled, and therefore, can be easily integrated in the industry [30].

The results of this study show that the plasticity of the Inconel alloy 625 can be further improved by more than 50% after the application of the electron beam treatment procedure, although the phase composition of the alloy was not transformed. However, it was already reported that the application of an electron beam treatment using the lower beam power of 600 W led to a transformation of the preferred crystallographic orientation and reorientation in the microvolumes, and therefore, the mobility of the dislocations within the new family of crystallographic planes and their corresponding directions should be higher, pointing to better plasticity. Thus, the reorientation of the microvolumes and the formation of a preferred crystallographic orientation should be considered reasons for the improvement in the plasticity of the electron-beam-surface-modified Inconel alloy 625.

From another point of view, the plasticity can be influenced not only by the crystallographic structure but also by the microstructure of the considered specimens. Since the plasticity of materials is strongly related to the slipping of dislocations, it is obvious that it could be reduced by the obstruction of their distribution and maintained with hard precipitates, second-phase structures, etc. [30,31]. Therefore, microstructures with the existence of precipitates that are capable of obstructing and limiting dislocation movement and slipping should be characterized by worsened plasticity. These statements are in agreement with the results of this study, where it was shown that the plasticity of the modified surface was improved after the application of electron beam surface modification with a beam power of 1200 W. Through the application of the aforementioned technological conditions and using a 1200 W power electron beam, the microstructure was significantly modified, and no precipitates could be observed within the modified zone. Therefore, no obstacles to the movement and distribution of the dislocations could be observed, meaning that the slipping of the dislocations could occur, pointing to a lower  $H^3/E^2$  ratio and, thus, a worse resistance to plastic deformation, and better plasticity. This could be considered a reason for the improvement in the plastic properties on the surface of the Inconel alloy 625.

As already mentioned, the results obtained in this study show that the plasticity of Inconel alloy 718 can be significantly improved (by more than 50%) by the application of an electron beam surface modification technology. This enhancement is higher than that reported by the authors of [18]. They showed that the plasticity of an Inconel alloy was improved by 41% via the application of a novel heat treatment approach, including higher-temperature homogenization and a lower-temperature aging treatment [18]. The results obtained in the present study concerning plasticity and plastic deformation demonstrated that the discussed mechanical characteristics can be greatly improved by the electron beam surface modification technology. This corresponds to an enhancement in the damping properties and a significant reduction in crack formation and initiation, which could open up a number of practical applications in modern industrial branches, such as aerospace, automotive, and others.

## 5. Conclusions

The results obtained in the present study show the possibility of electron beam modification of the structure and plasticity of Inconel alloy 625, where the beam power was chosen to be 600 and 1200 W. The following statements were deduced from the obtained data:

- The application of the electron beam surface modification of the Inconel alloy 625 led to the formation of a preferred crystallographic orientation in all the considered cases. The lower value of the beam power of 600 W did not lead to a significant change in

- the microstructure on the surface of the processed specimen. Increasing the power of the heat source led to the formation of a clearly distinguished modified zone.
- The application of the lower power of the electron beam of 600 W did not lead to a change in the hardness of the alloy. Using an electron beam with a higher output power led to structural changes in the alloy, such that the hardness of the alloy decreased from 3 to 2.5 GPa.
  - The Young's modulus increased from 100 to 153 GPa in the case of electron beam modification with the lower value of the beam power. Subsequently, treating the sample with the higher-power heat source led to a reduction in the Young's modulus to values closer to those of the untreated sample.
  - The results for the resistance to plastic deformation, i.e., the  $H^3/E^2$  ratio, show that it decreased in both cases after the surface treatment process by about 50%, which suggests that an improvement in the plasticity of the material was observed.

**Author Contributions:** Conceptualization, S.V. and S.P.; methodology, S.V., G.K., S.P., M.O., B.S., F.P. and I.P.; formal analysis, S.V., M.O., G.K., S.P., F.P., B.S. and I.P.; investigation, S.V., M.O., G.K., S.P., F.P., B.S. and I.P.; writing—original draft preparation, S.V. and G.K.; writing—review and editing, S.V.; visualization, F.P.; supervision, S.V. and I.P.; project administration, S.V. and I.P.; funding acquisition, S.V. and I.P. All authors have read and agreed to the published version of the manuscript.

**Funding:** This research was funded by the Bulgarian National Science Fund, grant number KP-06-N 67/7.

**Institutional Review Board Statement:** Not applicable.

**Informed Consent Statement:** Not applicable.

**Data Availability Statement:** Data are contained within the article.

**Acknowledgments:** Electron beam surface modification experiments were performed thanks to the research infrastructure of the “Centre of competence”—BG05M2OP001–1.002–0023–C01 “INTELLIGENT MECHATRONICS, ECO- AND ENERGY-SAVING SYSTEMS AND TECHNOLOGIES”.

**Conflicts of Interest:** The authors declare no conflicts of interest.

## References

1. Ivanov, Y.; Gromov, V.; Zaguliaev, D.; Konovalov, S.; Rubannikova, Y.; Semin, A. Prospects for the Application of Surface Treatment of Alloys by Electron Beams in State-of-the-Art Technologies. *Prog. Phys. Met.* **2020**, *21*, 345–362. [\[CrossRef\]](#)
2. Ivanov, Y.; Gromov, V.; Zagulyaev, D.; Konovalov, S.; Rubannikova, Y. Improvement of Functional Properties of Alloys by Electron Beam Treatment. *Steel Transl.* **2022**, *52*, 71–75. [\[CrossRef\]](#)
3. Filyakov, A.D.; Pochetukha, V.V.; Romanov, D.A.; Vashchuk, E.S. Influence of Electron Beam Treatment on Structure and Phase Composition of TiB<sub>2</sub>–Ag Coating Deposited by Electrical Explosion Spraying. *Coatings* **2023**, *13*, 1867. [\[CrossRef\]](#)
4. Klimov, A.S.; Bakeev, I.Y.; Dolgova, A.V.; Kazakov, A.V.; Korablev, N.S.; Zenin, A.A. Features of Electron Beam Processing of Mn-Zn Ferrites in the Fore-Vacuum Pressure Range in Continuous and Pulse Modes. *Coatings* **2023**, *13*, 1766. [\[CrossRef\]](#)
5. Zagulyaev, D.; Konovalov, S.; Gromov, V.; Glezer, A.; Ivanov, Y.; Sundeev, R. Structure and properties changes of Al-Si alloy treated by pulsed electron beam. *Mater. Lett.* **2018**, *229*, 377–380. [\[CrossRef\]](#)
6. Genk, Y.; Chen, X.; Konovalov, S.; Panchenko, I.; Ivanov, Y.; Deev, V.; Prusov, E. Ultrafast microstructure modification by pulsed electron beam to enhance surface performance. *Surf. Coat. Technol.* **2022**, *434*, 128226. [\[CrossRef\]](#)
7. Fu, Y.; Hu, J.; Shen, X.; Wang, Y.; Zhao, W. Surface hardening of 30CrMnSiA steel using continuous electron beam. *Nucl. Instrum. Methods Phys. Res. B* **2017**, *410*, 207–214. [\[CrossRef\]](#)
8. Konovalov, S.; Ivanov, Y.; Gromov, V.; Panchenko, I. Fatigue-induced evolution of AISI 310S steel microstructure after electron beam treatment. *Materials* **2020**, *13*, 4567. [\[CrossRef\]](#)
9. Rakhadilov, B.; Kengesbekov, A.; Zhurerova, L.; Kozhanova, R.; Sagdoldina, Z. Impact of electronic radiation on the morphology of the fine structure of the surface layer of R6M5 steel. *Machines* **2021**, *9*, 24. [\[CrossRef\]](#)
10. Zhao, G.; Sun, M.; Zhao, H.; Li, H.; Ma, L. Study on modification of 253 MA austenitic stainless steel by electron beam surface remelting treatment. *Surf. Coat. Technol.* **2023**, *470*, 129834. [\[CrossRef\]](#)
11. Valkov, S.; Parshorov, S.; Andreeva, A.; Rabadzhiyska, S.; Nikolova, M.; Bezdushnyi, R.; Petrov, P. Influence of beam power on the surface architecture and corrosion behavior of electron-beam treated Co-Cr-Mo alloys. *Nucl. Instrum. Methods Phys. Res. Sect. B* **2021**, *494–495*, 46–52. [\[CrossRef\]](#)

12. Kulka, M.; Makuch, N.; Dziarski, P. A study of nanoindentation for mechanical characterization of chromium and nickel borides' mixtures formed by laser boriding. *Ceram. Int.* **2014**, *40*, 6083–6094. [[CrossRef](#)]
13. Zhang, Y.; Jiang, Y.; Hu, X. Microstructure and high temperature creep properties of laser welded joints of Inconel 625 alloy formed by selective laser melting. *J. Weld.* **2020**, *41*, 78–84.
14. Paul, C.P.; Ganesh, P.; Mishra, S.K.; Bhargava, P.; Negi, J.; Nath, A.K. Investigating laser rapid manufacturing for Inconel-625 components. *Opt. Laser Technol.* **2007**, *39*, 800–805. [[CrossRef](#)]
15. Jones, R.; Ang, A.; Peng, D.; Champagne, V.K.; Michelson, A.; Birt, A. Modelling Crack Growth in Additively Manufactured Inconel 718 and Inconel 625. *Metals* **2023**, *13*, 1300. [[CrossRef](#)]
16. Zafar, F.; Emadinia, O.; Conceição, J.; Vieira, M.; Reis, A. A Review on Direct Laser Deposition of Inconel 625 and Inconel 625-Based Composites—Challenges and Prospects. *Metals* **2023**, *13*, 787. [[CrossRef](#)]
17. Xu, L.; Chai, Z.; Zhang, X.; Peng, B.; Zhou, W.; Chen, X. A new approach to improve strength and ductility of laser powder deposited Inconel 718 thin-wall structure. *Mater. Sci. Eng. A* **2022**, *885*, 143871. [[CrossRef](#)]
18. Li, X.; Shi, J.; Cao, G.; Russell, A.; Zhou, Z.; Li, C.; Chen, G. Improved plasticity of Inconel 718 superalloy fabricated by selective laser melting through a novel heat treatment process. *Mater. Des.* **2019**, *180*, 107915. [[CrossRef](#)]
19. Wang, X.; Ding, Y.; Gao, Y.; Ma, Y.; Chen, J.; Gan, B. Effect of grain refinement and twin structure on the strength and ductility of Inconel 625 alloy. *Mater. Sci. Eng. A* **2021**, *823*, 141739. [[CrossRef](#)]
20. Li, J.; Yao, J.; Zhao, G.; Li, H.; Li, Y.; Liu, J. The Influence of different focusing currents on the microstructure evolution and wear properties of a scanning electron beam modified Inconel 625 nickel base alloy surface. *Crystals* **2023**, *13*, 325. [[CrossRef](#)]
21. Valkov, S.; Parshorov, S.; Andreeva, A.; Bezdushnyi, R.; Nikolova, M.; Dechev, D.; Ivanov, N.; Petrov, P. Influence of Electron Beam Treatment of Co–Cr Alloy on the Growing Mechanism, Surface Topography, and Mechanical Properties of Deposited TiN/TiO<sub>2</sub> Coatings. *Coatings* **2019**, *9*, 513. [[CrossRef](#)]
22. Petrov, P.; Dechev, D.; Ivanov, N.; Hikov, T.; Valkov, S.; Nikolova, M.P.; Yankov, E.; Parshorov, S.; Bezdushnyi, R.; Andreeva, A. Study of the influence of electron beam treatment of Ti5Al4V substrate on the mechanical properties and surface topography of multilayer TiN/TiO<sub>2</sub> coatings. *Vacuum* **2018**, *154*, 264–271. [[CrossRef](#)]
23. Li, S.; Wei, Q.; Shi, Y.; Zhu, Z.; Zhang, D. Microstructure Characteristics of Inconel 625 Superalloy Manufactured by Selective Laser Melting. *J. Mater. Sci. Technol.* **2015**, *31*, 946–952. [[CrossRef](#)]
24. Angelov, V.; Ormanova, M.; Kaisheva, D.; Lazarova, R.; Dimitrova, R.; Petrov, P. Selective electron beam surface alloying of aluminum with TiCN nanoparticles. *Nucl. Instr. Meth. Phys. Res. Sec. B* **2019**, *440*, 88–94. [[CrossRef](#)]
25. Oliver, W.; Pharr, G. An improved technique for determining hardness and elastic modulus using load and displacement sensing indentation experiments. *J. Mater. Res.* **1992**, *7*, 564–1583. [[CrossRef](#)]
26. Oliver, W.; Pharr, G. Measurement of hardness and elastic modulus by instrumented indentation: Advances in understanding and refinements to methodology. *J. Mater. Res.* **2004**, *19*, 3–20. [[CrossRef](#)]
27. Leyland, A.; Matthews, A. On the significance of the H/E ratio in wear control: A nanocomposite coating approach to optimised tribological behavior. *Wear* **2000**, *246*, 1–11. [[CrossRef](#)]
28. Grabco, D.; Pyrtsac, C.; Shikimaka, O. Plasticity and resistance indices in Cu/soft substrate and Cu/hard substrate coated systems. *Rom. J. Phys.* **2023**, *68*, 602.
29. Zhang, P.; Zhang, L.; Baxevanakis, K.P.; Lu, S.; Zhao, L.G.; Bullough, C. Discrete crystal plasticity modelling of slip-controlled cyclic deformation and short crack growth under low cycle fatigue. *Int. J. Fatigue* **2021**, *145*, 106095. [[CrossRef](#)]
30. Zhu, Y.; Wu, X. Ductility and plasticity of nanostructured metals: Differences and issues. *Mater. Today Nano* **2018**, *2*, 15–20. [[CrossRef](#)]
31. Kawabata, T.; Izumi, O. The relationship between ductility and grain-boundary precipitates in an Al-6.0% Zn-2.6% Mg alloy. *J. Mater. Sci.* **1976**, *11*, 892–902. [[CrossRef](#)]

**Disclaimer/Publisher's Note:** The statements, opinions and data contained in all publications are solely those of the individual author(s) and contributor(s) and not of MDPI and/or the editor(s). MDPI and/or the editor(s) disclaim responsibility for any injury to people or property resulting from any ideas, methods, instructions or products referred to in the content.